CHEMISTRY
A EUROPEAN JOURNAL

DOI: 10.1002/chem.200500928

Electron-Rich Tetrathiafulvalene–Triarylamine Conjugates: Synthesis and Redox Properties

Hongchao Li and Christoph Lambert*[a]

Abstract: By combining tetrathiafulvalenes (TTFs) and triarylamines, four TTF–triarylamine conjugates bridged by an annulated pyrrole ring were designed and synthesized by an *N*-arylation reaction. Electrochemical and photophysical investigations suggest that these novel conjugates possess very strong electron-donating ability with very high HOMO energy levels of around −4.70 eV; the HOMOs are mainly located on the TTF moiety. We observed significant electronic coupling between the TTF moieties and the triarylamine groups. However, no evidence for such electronic communication between end-capping TTF units (conjugates **5** and **7**) or between two terminal triarylamine groups (conjugate **9**) could be found. Differential scanning calorimetry (DSC) measurements together with PM3-optimized geometries suggest that conjugates **5** and **7**, which adopt three-dimensional propeller-shaped structures, may easily pack and crystallize in the solid state because of the large rigid planar blades consisting of TTF and one of the phenyl rings of the triarylamine moiety. However, conjugate **9**, with two bulky end-capping triarylamine groups, forms an amorphous material with a glass transition at 74.5 °C.

Keywords: conducting materials · cyclic voltammetry · hole transfer · tetrathiafulvalene · triarylamines

Introduction

Since the first report on the synthesis and properties of organic metals based on tetracyano-*p*-quinodimethane (TCNQ) electron acceptors,[1] tetrathiafulvalene (TTF) and its derivatives have attracted extensive research interest as strong electron donors for the development of electrical conductors and superconductors.[2] To increase the electrical conductivity and dimensionality of charge-transfer materials, several chemical modifications have been carried out on the TTF skeleton: a) replacement of sulfur by other chalcogen atoms and introduction of more chalcogen atoms in the peripheral positions;[3] b) development of TTF analogues (known as extended TTFs) with extended π-conjugation bridges;[4] c) functionalization of TTF molecules with hydrogen- and halogen-bonding groups.[5] The aim of all of these strategies is to enhance the intermolecular orbital overlap by the formation of highly ordered stacks or even highly dimensional sheets induced by chalcogen–chalcogen interactions, π–π stacking or hydrogen- and halogen-bonding interactions. Besides the significant research efforts on developing molecular organic metals, TTF and its derivatives are used as building blocks in macromolecular and supramolecular systems for various applications,[6] such as chemical sensors,[7] molecular switches,[8] molecular shuttles,[9] organic ferromagnets,[10] molecular rectifiers,[11] molecular transistors,[12] nonlinear optical materials,[13] and photovoltaic materials.[14]

Due to the electron-donating nature of the nitrogen atom, triarylamines are widely used as hole-transporting materials for various applications, such as xerography, light-emitting diodes, solar cells, organic field-effect transistors, photorefractive systems, and so on.[15] On the other hand, amorphous materials, especially amorphous organic molecular materials, have recently attracted a great deal of attention as a new class of materials because of their good processability, transparency, and homogeneous properties. Low molecular weight species in particular are promising because of the ease with which amorphous films can be formed, either by vacuum deposition or by spin coating from solution.[16] Triarylamines not only possess a particularly strong electron-donating nature, but also a three-dimensional propeller blade structure that inherently favors an amorphous solid state due to the existence of rotational isomers.[17] Thus, based upon triarylamines, a variety of nonplanar "starburst" amorphous organic molecular materials have been developed and thoroughly investigated.[18] Such molecular glasses

[a] Dr. H. Li, Prof. Dr. C. Lambert
Institut für Organische Chemie
Bayerische Julius-Maximilians-Universität Würzburg
Am Hubland, 97074 Würzburg (Germany)
Fax: (+49) 931-888-4606
E-mail: lambert@chemie.uni-wuerzburg.de

WILEY InterScience DISCOVER SOMETHING GREAT
© 2006 Wiley-VCH Verlag GmbH & Co. KGaA, Weinheim

are characterized by low ionization potentials of 5.0 to 5.1 eV,[16a] by reversible anodic oxidation to form stable radical cations, and by the excellent quality of their amorphous thin films prepared by vacuum deposition or spin coating from solution. As a result of these properties, these materials are ideal for use as hole-transporting layers in electro-optical applications.

Based on the facts that: a) TTF and its derivatives possess an even stronger electron-donating ability than triarylamines and that TTFs can be sequentially and reversibly oxidized to radical cations and dications at quite low potentials;[19] and b) triarylamines possess a unique propeller-shaped architecture that allows them to be used as high-dimensional scaffolds, and a high reactivity at the *para* positions,[20] the combination of TTF chemistry with arylamine chemistry could be expected to provide an opportunity to develop high-dimensional molecular conductors and/or amorphous hole-injection and transport molecular materials with advanced material properties. Herein, we report a first study to introduce TTFs in combination with triarylamines into a non-classical but promising field of amorphous molecular materials, with a view to potential applications of these systems as charge-transporting materials in optoelectronic devices.

Results and Discussion

Synthesis of TTF–triarylamine conjugates: The combination of pyrrole-annulated TTFs (**1** and **8**)[21] with triarylamine units (**2**, **4**, and **6**) was realized by an *N*-arylation reaction of the pyrrole moiety of **1** or **8**, respectively, as outlined in Scheme 1. Applying the copper catalyst system reported by Buchwald,[22] we obtained compound **3** with one TTF branch, **5** with two TTF branches, and **7** with three TTF branches by *N*-arylation of **1** with compounds **2**, **4**, and **6**, respectively. Similarly, the dumbbell compound **9** with two terminal arylamine units linked by the TTF skeleton was also prepared in reasonable yield by *N*-arylation of **8** with two equivalents of compound **2**. ^{1}H NMR, ^{13}C NMR, and MALDI MS were used to characterize the new TTF–triarylamine conjugates.

Electrochemistry: The electrochemical properties of the TTF–triarylamine conjugates **3**, **5**, **7**, and **9** were investigated by cyclic voltammetry (CV) and differential pulse voltammetry (DPV) experiments (Figure 1 and Figure 2). For comparison, cyclic voltammograms of intermediates **1**, **8**, and bis(4-methoxyphenyl)-*N*-phenylamine (**TAA**) were also obtained under the same conditions; all data are listed in Table 1. As shown in Figure 1, conjugate **3** displays three reversible one-electron anodic redox couples, which correspond to the sequential removal of electrons from the TTF and triarylamine moieties to form the radical cation, dication, and trication. Compared with the CVs of intermediates **1** and **TAA**, the first low-potential redox couple at −0.01 V fits well with that of **1** ($E^1_{1/2} = -0.02$ V), suggesting that the first electron is removed from the TTF unit and that the attached arylamino group has little effect on the first oxidation potential of TTF. The other two redox couples occur at 0.30 V and at 0.49 V. Here, we assign the second couple to the oxidation of the arylamino moiety and the third one to the formation of the dication TTF^{2+}. This assignment was confirmed by chemical redox titration and spectroelectrochemistry as described below. Compared with the oxidation of **TAA** ($E_{1/2} = 0.35$ V), the second redox couple (related to the triarylamine unit) is at a somewhat lower potential, which might be due to the attached electron-donating $TTF^{+\cdot}$ moiety (which is still an electron donor ready to lose the second electron to form aromatic TTF^{2+}). However, compared with the second oxidation of TTF **1**$^{+\cdot}$ ($E^2_{1/2} = 0.41$ V), the third redox couple of **3** ($E^3_{1/2} = 0.53$ V) has a potential slightly more positive than that of **TAA**$^{+\cdot}$. Correspondingly, DPV of **3** displays three one-electron oxidations at −0.01 V, 0.29 V, and 0.47 V (Figure 2), which are comparable to the corresponding $E_{1/2}$ values obtained by CV. The HOMO energy level of **3**, which can be deduced from the CV potential for the onset of oxidation, was estimated to be −4.75 eV by taking the HOMO level of ferrocene as −4.8 eV.[15a,23] This value is very close to that of TTF **1** ($E_{HOMO} = -4.74$ eV) and much higher than that of **TAA** ($E_{HOMO} = -5.03$ eV),[24] indicating that the HOMO of conjugate **3** is mainly located on the more strongly electron-donating TTF part.

With two TTF branches, conjugate **5** shows three fully reversible redox couples at −0.02 V, 0.42 V, and 0.61 V in its CV. The first and second couples cover two unresolved oxidation processes each, indicating that two electrons are almost simultaneously removed from the two TTF groups to form two $TTF^{+\cdot}$ in **5**$^{2+}$, and that two further electrons are again almost simultaneously removed from the two $TTF^{+\cdot}$ at a higher potential to form two TTF^{2+} in **5**$^{4+}$. More interestingly, the first and second redox couples are at almost the same potentials as those of intermediate TTF **1**, except that the redox couples of **5** show two-electron behavior. Based on the above CV, there is no significant electronic communication between the two TTF branches, which is due to the nonplanar propeller-shape of the triarylamine bridge. In comparison with the triarylamine oxidation of **3** ($E^2_{1/2} = 0.30$ V) and of **TAA** ($E_{1/2} = 0.35$ V), the arylamine unit in **5** is oxidized at a much more positive potential ($E^3_{1/2} = 0.61$ V). This is not surprising given the direct π-conjugation path between the TTF branch and the arylamine group via the aromatic pyrrole ring. Thus, the electron-withdrawing TTF^{2+} dications render the removal of an electron from the arylamine more difficult. Similarly, the DPV investigation also suggests that the oxidation of the triarylamine shifts to a higher potential (0.61 V versus Fc/Fc^{+}) due to the electron-withdrawing TTF^{2+} moiety. The calculated HOMO ($E_{HOMO} = -4.76$ eV) is comparable with that of intermediate TTF **1**.

The CV and DPV characterize the electrochemistry of conjugate **7** with three TTF moieties by three reversible redox couples ($E^1_{1/2} = 0.00$ V, $E^2_{1/2} = 0.46$ V, and $E^3_{1/2} = 0.94$ V); the first two couples comprise three unresolved

 © 2006 Wiley-VCH Verlag GmbH & Co. KGaA, Weinheim

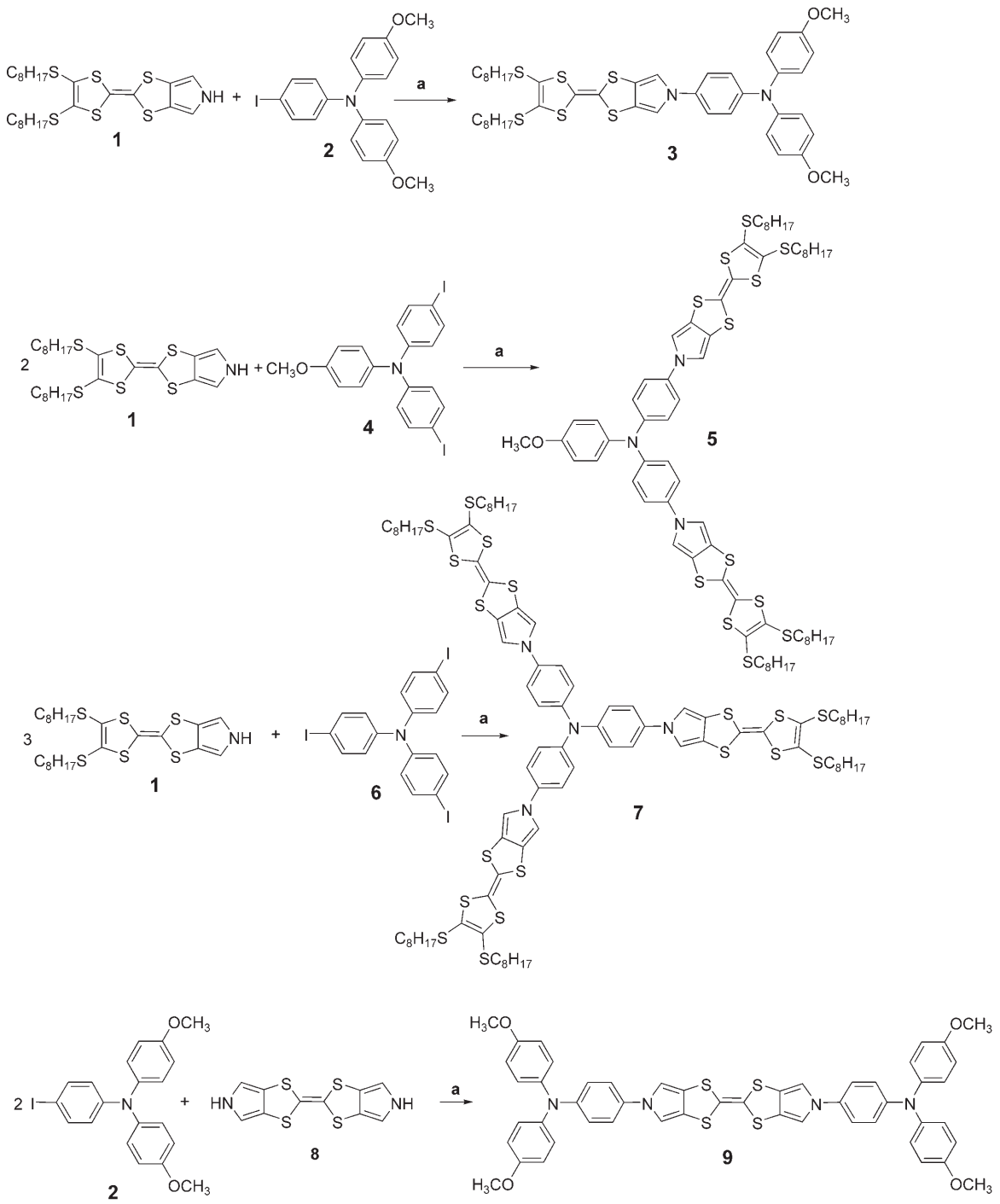

Scheme 1. Synthesis of TTF–triarylamine conjugates **3**, **5**, **7**, and **9**. Reagents and conditions: a) CuI, K_3PO_4, *trans*-cyclohexanediamine, dioxane, 110 °C, 24 h.

redox processes, and the last one shows single-electron behavior. Similarly to **5**, the first two three-electron couples can be assigned to the almost simultaneous oxidation of TTF branches as explained above for compound **5**. There is no evidence of significant electronic communication between the three TTF branches. The attachment of the formed TTF^{2+} to all three blades of the triarylamine shifts the oxidation of the arylamine center to an even more positive potential ($E^3_{1/2} = 0.94$ V) than in **5**. From the potential for the onset of oxidation, the HOMO of **7** can be estimated to be around −4.79 eV, which is comparable to those of TTF **1** and the conjugates **3** and **5**.

The dumbbell compound **9** shows significantly different electrochemistry. As displayed in Figure 1, the CV of **9** is characterized by three reversible redox couples at −0.06 V, 0.30 V, and 0.58 V. The first and the third couple were found

 © 2006 Wiley-VCH Verlag GmbH & Co. KGaA, Weinheim

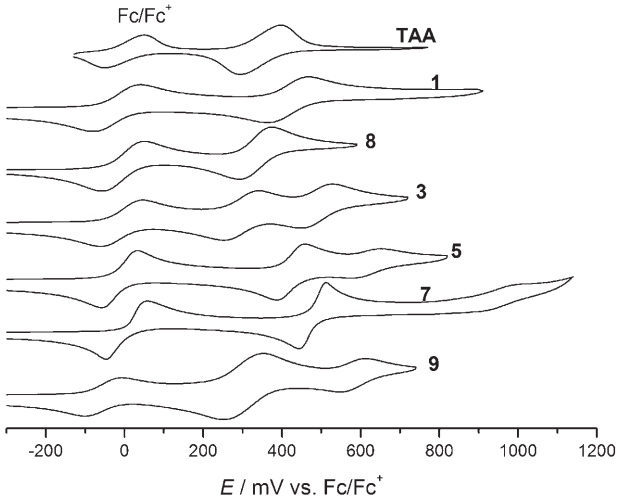

Figure 1. Cyclic voltammograms of TTFs (**1** and **8**), triarylamine **TAA**, and conjugates **3**, **5**, **7**, and **9** in $TBAPF_6/CH_2Cl_2$ at room temperature at a scan rate of 100 $mV\,s^{-1}$.

Table 1. Oxidation potentials and HOMO energy level of TTFs (**1** and **8**), triarylamine (**TAA**), and conjugates (**3**, **5**, **7**, and **9**) as determined by CV and DPV (in parentheses).[a]

Compd	$E^1_{1/2}$ [V][b]	$E^2_{1/2}$ [V][b]	$E^3_{1/2}$ [V][b]	E_{onset} [V]	HOMO [eV][c]
TAA	0.35	–	–	0.28	−5.08
1	−0.02	0.41	–	−0.06	−4.74
8	0.00	0.33	–	−0.05	−4.75
3	−0.01	0.30	0.49	−0.05	−4.75
	(−0.01)	(0.29)	(0.47)		
5	−0.02[d]	0.42[d]	0.61	−0.04	−4.76
	(0.01)	(0.43)	(0.61)		
7	0.00[e]	0.46[e]	0.94	−0.01	−4.79
	(−0.02)	(0.46)	(0.94)		
9	−0.06	0.30[d]	0.58	−0.10	−4.70
	(−0.04)	(0.30)	(0.57)		

[a] Conditions: potential versus Fc/Fc^+, Bu_4NPF_6 (0.1 M in acetonitrile), scan rate 100 $mV\,s^{-1}$ (for CV) and 20 $mV\,s^{-1}$ (for DPV). [b] $E_{1/2}$ determined from $(E_{pa} + E_{pc})/2$, where E_{pa} and E_{pc} refer to the peak potential in the anodic and cathodic scans, respectively. [c] The HOMO energy level was calculated from the onset potential of oxidation according to the empirical equation $E_{HOMO} = -e(E_{onset} + 4.8)$ V by assuming the energy level of ferrocene to be −4.8 eV below vacuum level. [d] Two-electron oxidation. [e] Three-electron oxidation.

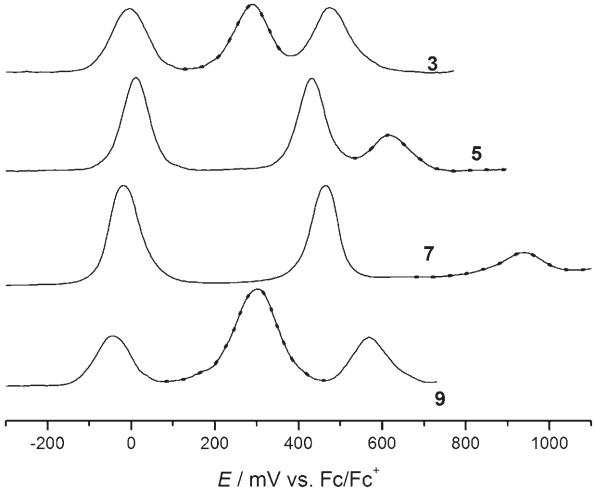

Figure 2. Differential pulse voltammograms of compounds **3**, **5**, **7**, and **9** in $TBAPF_6/CH_2Cl_2$ at room temperature at a scan rate of 20 $mV\,s^{-1}$. Redox couples associated with oxidation of the triarylamine unit are marked with dots.

to correspond to one-electron redox processes, while the second oxidation covers two unresolved redox processes. By comparison with the CVs of intermediate TTF **1**, **8**, and conjugate **3**, the first one-electron couple can be assigned to $TTF/TTF^{+\bullet}$, which is shifted towards a more negative potential due to the terminal electron-donating triarylamine units. This trend is also reflected by the calculated higher HOMO level (−4.70 eV). The subsequent two-electron oxidation is ascribed to the simultaneous removal of two electrons from the two arylamine endgroups, again indicating that there is no significant electronic coupling between the terminal arylamine units through the TTF^+ bridge. The sequentially formed $TTF^{+\bullet}$ and $TAA^{+\bullet}$ make the second oxidation of the central TTF unit much more difficult (0.58 V) in comparison with the corresponding redox couples of **1** ($E^2_{1/2} = 0.41$ V), **8** ($E^2_{1/2} = 0.33$ V), and **3** ($E^3_{1/2} = 0.49$ V).

As discussed above, the first low oxidation potential of all TTF–triarylamine conjugates (**3**, **5**, **7**, and **9**) is attributed to the strongly electron-donating TTF moiety, and all of the calculated HOMO energy levels (between −4.70 eV and −4.80 eV) are much higher than those of arylamines (−5.0 to −5.10 eV), which have been widely reported as hole-injection and transport materials.[16a] In view of the fact that the normally used anodic indium tin oxide (ITO) possesses a work function of around −4.70 eV, the TTF–triarylamine conjugates **3**, **5**, **7**, and **9** presented in this work match the ITO work function very well and might be promising as active molecular materials for electro-optical devices.

UV/Vis-NIR spectra of TTF-triarylamine radical cations: The spectral properties of the neutral and oxidized compounds **3**, **5**, **7**, and **9** were analyzed by UV/Vis-NIR absorption spectroscopy using $SbCl_5$ as the oxidant in dichloromethane. The spectra were compared with those of intermediates **1** (shown in Figure 3), **8**, and **TAA**. The most relevant photophysical data are collected in Table 2.

Figure 3 shows UV/Vis-NIR spectra of TTF **1** treated with increasing amounts of the oxidant $SbCl_5$ in CH_2Cl_2. The neutral **1** displays its maximum absorption at around 30600 cm^{-1}, with a long tail extending into the visible region. The following chemical titration experiment suggests that TTF was first reversibly oxidized to its radical cation ($TTF^{+\bullet}$) and then to the dication, which was confirmed by changes in the absorption spectra and the clear isobestic points in Figure 3a,b. As shown in Figure 3a, with the addition of the oxidant $SbCl_5$, the newly emerging absorption peaks at 23100 cm^{-1} and 12400 cm^{-1}, which we assign to $TTF^{+\bullet}$, continue to increase. The former transition is characteristic of this type of $TTF^{+\bullet}$, while the latter band is inter-

 © 2006 Wiley-VCH Verlag GmbH & Co. KGaA, Weinheim

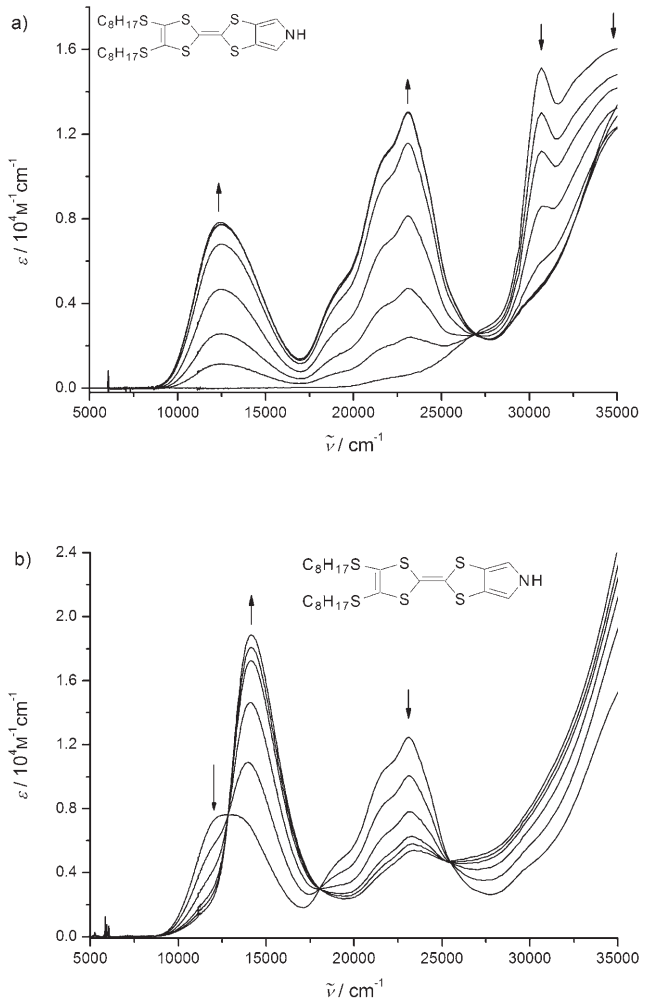

Figure 3. Chemical oxidant titration curves of TTF **1** in CH_2Cl_2. From a) to b), the absorption spectra of **1** treated with increasing amounts of oxidant show three phases. The arrows indicate increasing addition of the oxidant.

Table 2. Photophysical data from chemical oxidant titrations of TTF **1**, triarylamine **TAA**, and conjugates **3**, **5**, **7**, and **9**.[a]

Compd	$\tilde{\nu}_{neu}$ [cm^{-1}][b] (ε, 10^4 M^{-1}cm^{-1})	$\tilde{\nu}_{ox1}$ [cm^{-1}][c]	$\tilde{\nu}_{ox2}$ [cm^{-1}][d]	$\tilde{\nu}_{ox3}$ [cm^{-1}][e]	E_g [eV]	LUMO [eV][f]
TAA	33500 (2.3)	28900, 14100	–	–	–	–
1	30600 (1.4)	23100, 12400	14200	–	–	–
3	32300 (3.0), 29700 (3.7)	22700, 13200, 8900	26300, 22700, 13000, 10000	27500, 12600	3.25	−1.41
5	32300 (5.4), 29700 (7.2)	22800, 13600, 9800	14100, 8700	26500, 12800	3.20	−1.47
7	32300 (5.8), 29300 (9.8)	23600, 14600, 10400	14100, 10300	–[g]	3.17	−1.58
9	32300 (4.5), 29300 (5.5)	22100, 15700, 10500, 8100	26600, 22200, 13000, 9000	26600, 13000	3.25	−1.39

[a] A solution of the compound in CH_2Cl_2 (2×10^{-5} M) was titrated with a solution of $SbCl_5$ in CH_2Cl_2. [b] The maximum absorption of the neutral compound. [c] The maximum absorption of the oxidized compound in the first phase of the titration. [d] The maximum absorption of the oxidized compound in the second phase of the titration. [e] The maximum absorption of the oxidized compound in the third phase of the titration. [f] LUMO level calculated from the equation $E_{LUMO} = E_g + E_{HOMO}$. [g] No significant change in absorption with further addition of oxidant.

preted to be of charge-resonance type (HOMO → SOMO).[25] Upon further addition of oxidant, the absorptions due to $TTF^{+\cdot}$ start to decrease and a new absorption peak appears at 14200 cm^{-1}, which can be ascribed to TTF^{2+}.

Compound **3**, which comprises one TTF group and one triarylamine group, exhibits maximum absorption at 29700 cm^{-1}, with a shoulder at 32300 cm^{-1} in the UV region (see Figure 4). The absorption is estimated to start at 26100 cm^{-1}, and the corresponding HOMO–LUMO gap E_g = 3.26 eV can be deduced from the onset absorption of neutral **3**. With increasing addition of oxidant $SbCl_5$, the absorption of the solution of **3** decreases in the UV region. Simultaneously, three new absorption peaks appear at 22700, 13200, and 9100 cm^{-1}. By comparison with the spectrum of oxidized TTF intermediate **1** ($TTF^{+\cdot}$, 23100 and 12400 cm^{-1}), the absorptions at 22700 and 9100 cm^{-1} can again be assigned to TTF^{+}. The less intense shoulder absorption at 13200 cm^{-1} may be due to optically induced hole transfer from $TTF^{+\cdot}$ to the triarylamine moiety. Further addition of oxidant yields $\mathbf{3}^{2+}$ with new absorption peaks at 26300 and 13000 cm^{-1}, which are similar to the absorptions of the triarylamine radical cation ($\mathbf{TAA}^{+\cdot}$, 28000 and 14000 cm^{-1}).[26] Finally, the second oxidation of the TTF group was accomplished, as indicated by a decrease of the characteristic $TTF^{+\cdot}$ absorption and an increase of the TTF^{2+} absorption at 12600 cm^{-1}. The absorption titration investigations outlined above confirm our rational assignment of the redox couples in the CV of **3**.

Compound **5**, with two TTF branches, displays a similar absorption spectrum to that of **3**, with the onset of absorption at 25700 cm^{-1} (Figure 5). Treatment with oxidant gives two intense absorptions at 22800 cm^{-1} and 9800 cm^{-1}, which originate from the $TTF^{+\cdot}$ group. Simultaneously, a hole-transfer band (from $TTF^{+\cdot}$ to the triarylamine) is found at 13500 cm^{-1}. It should be noted that there is no visible intervalence charge-transfer band (IV-CT) that might originate from hole transfer from $TTF^{+\cdot}$ of one branch to the neutral TTF of the other branch, which confirms that there is no significant electronic communication between the two TTF branches. However, upon further oxidation, the absorption of $TTF^{+\cdot}$ decreases while two new absorption peaks at 14100 and 8700 cm^{-1} intensify. These bands are typical of TTF^{2+}. The same conclusion was drawn from the CV of **5** above. The simultaneous increase in the absorption at 8700 cm^{-1} might indicate hole transfer from TTF^{2+} to the triarylamine. This hole-transfer band has a lower energy compared with that of $TTF^{+\cdot}$ to triarylamine (13200 cm^{-1} in

 © 2006 Wiley-VCH Verlag GmbH & Co. KGaA, Weinheim

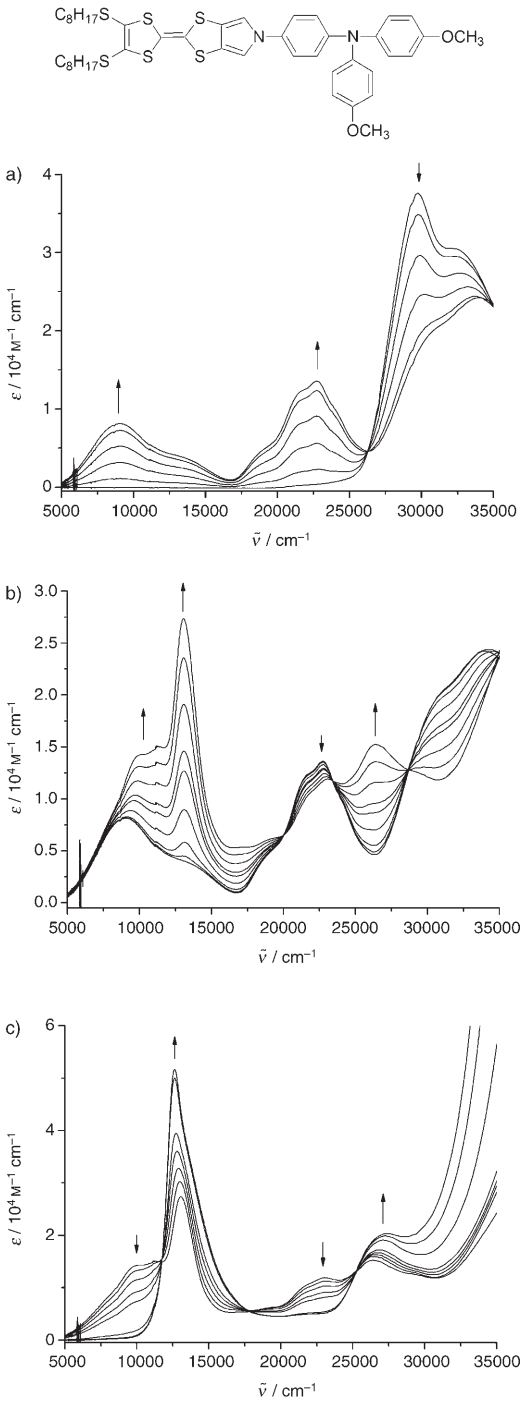

Figure 4. Chemical oxidant titration curves of compound **3** in CH_2Cl_2. From a) to c), the absorption spectra of **3** treated with increasing amounts of oxidant show four phases. The arrows indicate increasing addition of the oxidant.

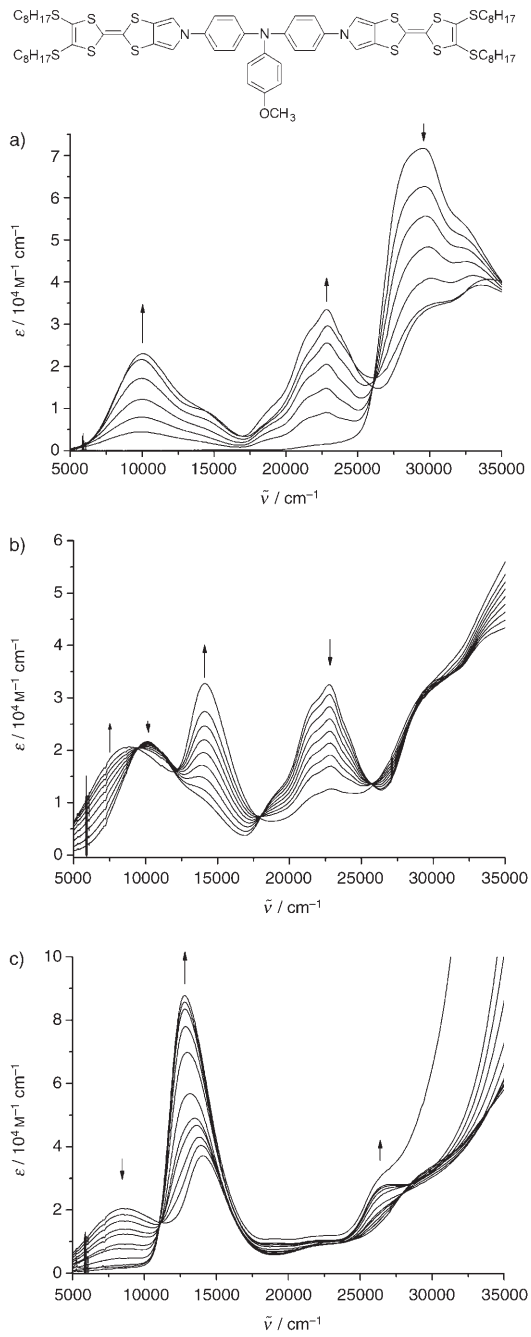

Figure 5. Chemical oxidant titration curves of compound **5** in CH_2Cl_2. From a) to c), the absorption spectra of **5** treated with increasing amounts of oxidant show four phases. The arrows indicate the increasing addition of the oxidant.

3^{+}). Upon addition of a further amount of oxidant, the triarylamine group was oxidized to the corresponding radical cation, which is consistent with the increasing absorptions at 26500 and 12800 cm^{-1} (assigned to the triarylamine radical cation) and the decreasing peak at 8700 cm^{-1} (hole-transfer band from TTF^{2+} to triarylamine).

The neutral star-shaped compound **7** with three TTF groups shows a comparable absorption spectrum to those of **3** and **5**. As shown in Figure 6, the corresponding E_g = 3.17 eV was estimated from the onset absorption of 25600 cm^{-1}. Upon oxidation, **7** shows two intense absorption bands in the visible region ($\tilde{\nu}_{max}$ = 23600 cm^{-1}) and near-IR region ($\tilde{\nu}_{max}$ = 10400 cm^{-1}), and one hole-transfer band at 14600 cm^{-1}. Upon further addition of oxidant, the absorp-

 © 2006 Wiley-VCH Verlag GmbH & Co. KGaA, Weinheim

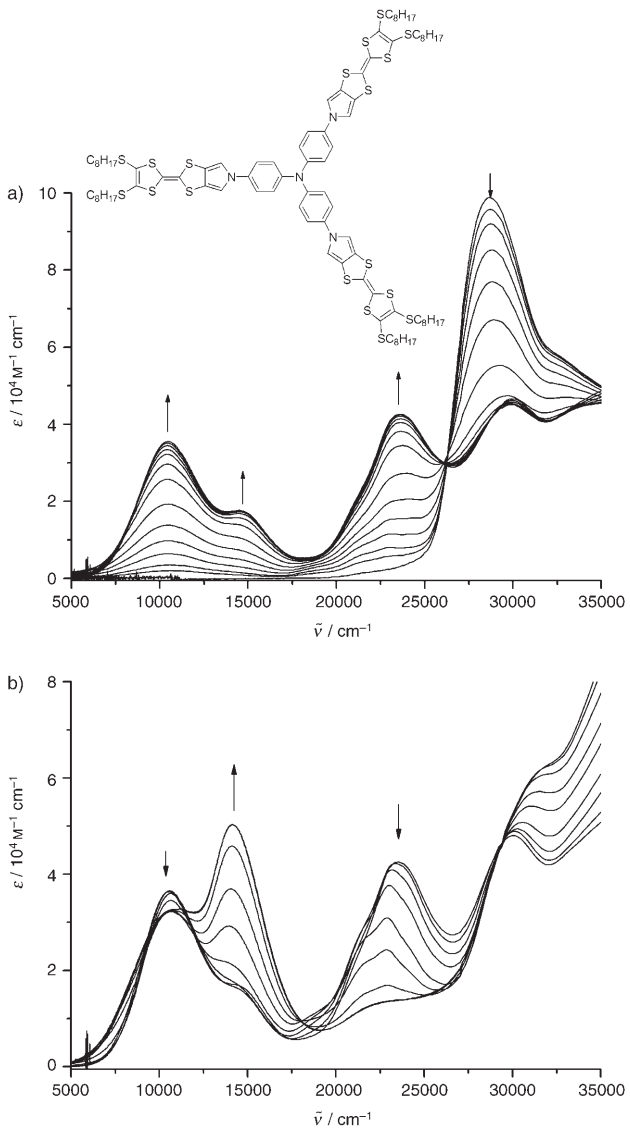

Figure 6. Chemical oxidant titration curves of compound **7** in CH_2Cl_2. From a) to b), the absorption spectra of **7** treated with increasing amounts of oxidant show three phases. The arrows indicate increasing addition of the oxidant.

tion associated with $TTF^{+\bullet}$ decreases while a new absorption peak emerges at 14100 cm^{-1}, which is related to TTF^{2+}. Along with the increase in the TTF^{2+} absorption and decrease in the $TTF^{+\bullet}$ absorption, the peak at around 10400 cm^{-1} decreases somewhat and then appears to be unchanged, which might be due to the overlapping $TTF^{+\bullet}$ absorption and hole-transfer (from TTF^{2+} to triarylamine) absorption band. In contrast to what was seen for **5**, further addition of oxidant did not result in any significant changes in the absorptions of **7**, although a further oxidation of triarylamine would be expected to decrease the hole-transfer band and to generate a triarylamine radical cation absorption band in the visible region (see spectroelectrochemistry studies below). Taking into account the very high oxidation potential of the arylamine group in **7** (E^3_{pa} = 0.98 V versus Fc/Fc^+), the oxidation potential of $SbCl_5$ might be insufficient to remove an electron from the arylamine core or the oxidation process might be too slow to detect changes in the spectra on our experimental time scale.

As shown in Figure 7, the spectrum of the dumbbell compound **9** is characterized by a strong absorption at 29300 cm^{-1} with a shoulder at 32300 cm^{-1}. An E_g of 3.25 eV, which is comparable to that of **3**, was determined from the lower energy absorption. Upon the addition of oxidant, the spectrum is characterized by increasing absorptions in the visible and NIR regions. As before, the fine-structured absorption at 22100 cm^{-1} can be ascribed to $TTF^{+\bullet}$. After deconvolution into Gaussian functions, the absorptions in the visible and NIR regions were found to comprise three peaks at 7900, 11000, and 15800 cm^{-1} (Figure 8). The two lower energy absorptions could be assigned to $TTF^{+\bullet}$, and the higher energy band at 15800 cm^{-1} might originate from a degenerate hole transfer from the central $TTF^{+\bullet}$ to the two triarylamine endgroups. In this way, $\mathbf{9}^+$ represents a symmetrical mixed-valence species in which the bridge is oxidized.[27] Upon further oxidation, the absorptions of $TTF^{+\bullet}$ are found to be saturated and new absorptions of the triarylamine radical cations at 13000 and 26600 cm^{-1} increase. It is interesting to note that the lower energy absorption peak of $TTF^{+\bullet}$ shifts slightly towards higher energy and its intensity is enhanced. These changes are caused by the oxidation of the terminal triarylamine units. Further oxidation of $TTF^{+\bullet}$ to its dication (13000 cm^{-1}) is responsible for the decrease in the $TTF^{+\bullet}$ absorption. Unfortunately, the intensity of the absorption of the fully oxidized **9** decreased because of its low solubility in the less polar solvent (a precipitate formed upon further addition of oxidant). During the titration, no IV-CT band between the two terminal triarylamine redox centers was detected, confirming that there is no significant electronic communication between them. Again, the results are in agreement with the assignment of the redox couples of **9** in the CV section.

Spectroelectrochemistry studies: To complement the results of the chemical oxidation of **7**, we carried out spectroelectrochemistry investigations at controlled applied potentials in $TBAPF_6/CH_2Cl_2$ solution.

The spectroelectrochemical investigation of star-shaped compound **7** provided more details than the corresponding chemical oxidant titration study because of the limited oxidation potential of the oxidant $SbCl_5$ or the rather slow oxidation rate achieved. As depicted in Figure 9, the absorptions of $TTF^{+\bullet}$ appear in the lower energy region (24000, 15000, and 11100 cm^{-1}) by applying a potential of 0.2 V ($E^1_{pa} < E < E^2_{pa}$). When the potential is increased to 0.7 V ($E^2_{pa} < E < E^3_{pa}$), the absorptions of $TTF^{+\bullet}$ diminish and the spectrum is characterized by a new peak at around 14400 cm^{-1} with a lower energy shoulder (11700 cm^{-1}). This is in agreement with the results of CV and the chemical oxidant titration, indicating that $TTF^{+\bullet}$ is oxidized to the corresponding dication TTF^{2+}. Along with the increase in oxidation potential to 1.1 V ($> E^3_{pa}$), the corresponding hole-

 © 2006 Wiley-VCH Verlag GmbH & Co. KGaA, Weinheim

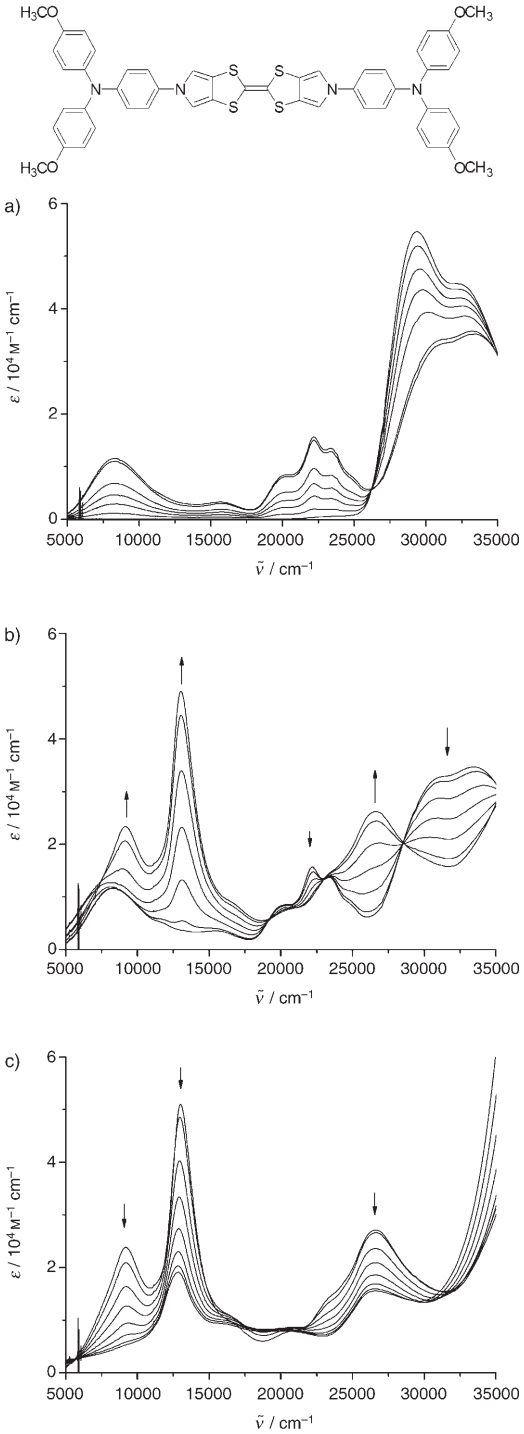

Figure 7. Chemical oxidant titration curves of compound **9** in CH_2Cl_2. From a) to c), the absorption spectra of **9** treated with increasing amounts of oxidant show four phases. The arrows indicate increasing addition of the oxidant. Note that precipitation of $\mathbf{9}^{4+}$ in c) results in a decrease in absorption over the whole UV/Vis-NIR region.

transfer band at 11700 cm^{-1} between TTF^{2+} and the triarylamine core disappears and a strong absorption located at 12800 cm^{-1} suggests that the central arylamine unit is oxidized.

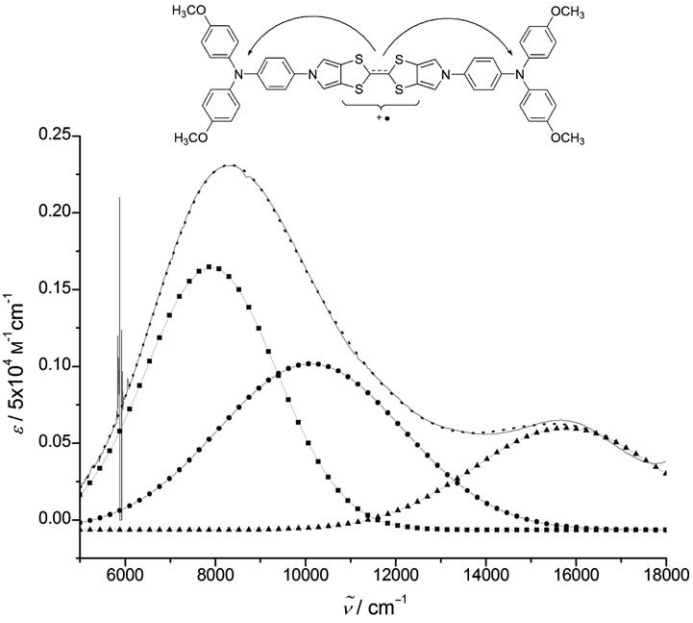

Figure 8. UV/Vis-NIR spectrum of $\mathbf{9}^{+\cdot}$ measured in CH_2Cl_2 (solid line). The spectrum was deconvoluted into Gaussian functions (line + symbol). The sum of the symbol lines (dotted lines) matches the measured spectrum.

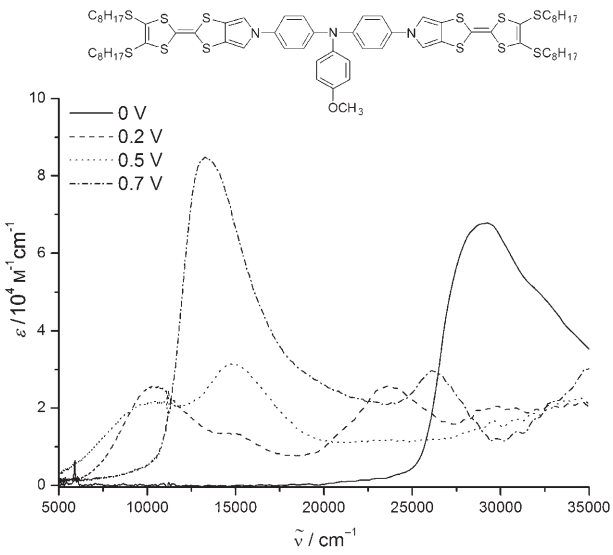

Figure 9. Spectroelectrochemical measurements on **5** in CH_2Cl_2.

Taking into account the effect of the electrolyte ($TBAPF_6$), the results of the spectroelectrochemistry investigations are consistent with those of the chemical oxidant titration experiments and prove that the missing triarylamine radical cation signal in the chemical oxidation experiment is due to either slow oxidation kinetics or the low oxidation potential of $SbCl_5$.

It should be noted that no fluorescence is observed from these TTF–triarylamine conjugates, indicating that the TTF moiety acts as an efficient quencher of fluorescence from the arylamine system. In fact, this fluorescence quenching

 © 2006 Wiley-VCH Verlag GmbH & Co. KGaA, Weinheim

effect of TTF has been attributed to its strong electron-donating properties.[28]

Differential scanning calorimetry studies: The thermal behavior of the TTF–triarylamine conjugates was studied by differential scanning calorimetry (DSC). To eliminate the thermal history of the samples, the second heating scans were recorded; the results are presented in Figure 10. Because conjugate **3** was obtained as a thick yellow oil, only compounds **5**, **7**, and **9** were investigated by DSC. As shown in the figure, compound **5** with two rigid TTF arms shows only a sharp, clear endothermic peak at around 115.7 °C, which is comparable to the melting point measured using a Büchi melting point apparatus (m.p. 114–115 °C). The DSC curve of conjugate **7** suggests no glass transition, and the corresponding melting point increases to 162.6 °C (the measured melting point is 159–160 °C). Although the triarylamine core endows compounds **5** and **7** with a three-dimensional propeller-like structure, the large, rigid, and planar propeller blades, which consist of a TTF unit and one phenyl ring of the triarylamine moiety, allow the molecules to crystallize. However, this is not the case for the dumbbell-shaped conjugate **9**. The DSC curve shows that **9** forms a molecular organic glass with a clear glass transition T_g = 74.5 °C. In fact, only a strong glass transition at 66.6 °C was seen in the first heating scan, and no crystallization transition was observed during the cooling scan. This is not too surprising because the two bulky propeller-shaped triarylamine groups prevent favorable intermolecular interactions between the rigid TTF moieties (packing of molecules) and hence prevent the molecule (conjugate **9**) from crystallizing.

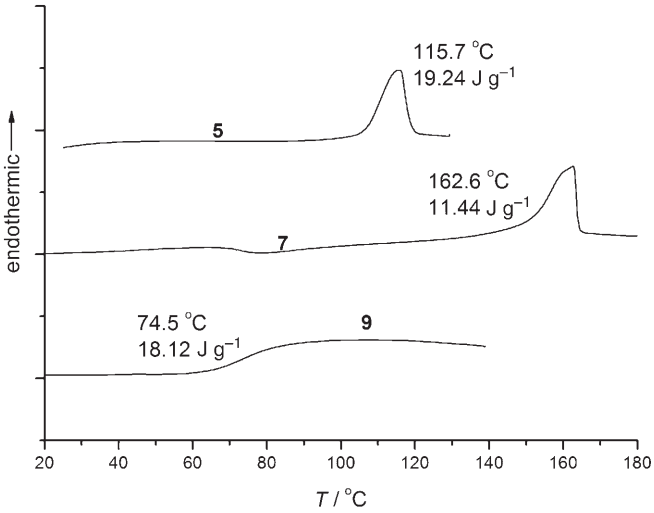

Figure 10. Differential scanning calorimetry of **5**, **7**, and **9**. Second heating scans at a scan rate of 10 °C min^{-1}.

Optimized geometries and calculated HOMO energy level: To gain insight into the conformation of the TTF-triarylamine conjugates **3**, **5**, **7**, and **9**, and to elucidate their electronic structure, quantum chemical calculations were performed by the semi-empirical PM3 method using Chem3D MOPAC. The highest occupied molecular orbital was also estimated using the PM3-optimized geometries.

As expected, the optimized geometries in Figure 11 show that the triarylamine groups adopt a three-dimensional propeller conformation in all cases. On the other hand, the rigid TTF moiety is in each case almost coplanar with the adjacent phenyl ring of the triarylamine forming a planar propeller blade.

The corresponding HOMO of the TTF-arylamine conjugates is mainly located on the TTF part (Figure 11 a,d), which is consistent with the TTF group being most easily oxidized.

Conclusion

Four pyrrole-bridged TTF-triarylamine conjugates (**3**, **5**, **7**, and **9**) were synthesized in reasonable yield by *N*-arylation of pyrrole-annulated TTFs **1** or **8**. The electrochemistry of the conjugates has been studied by means of cyclic voltammetry and differential pulse voltammetry. The respective

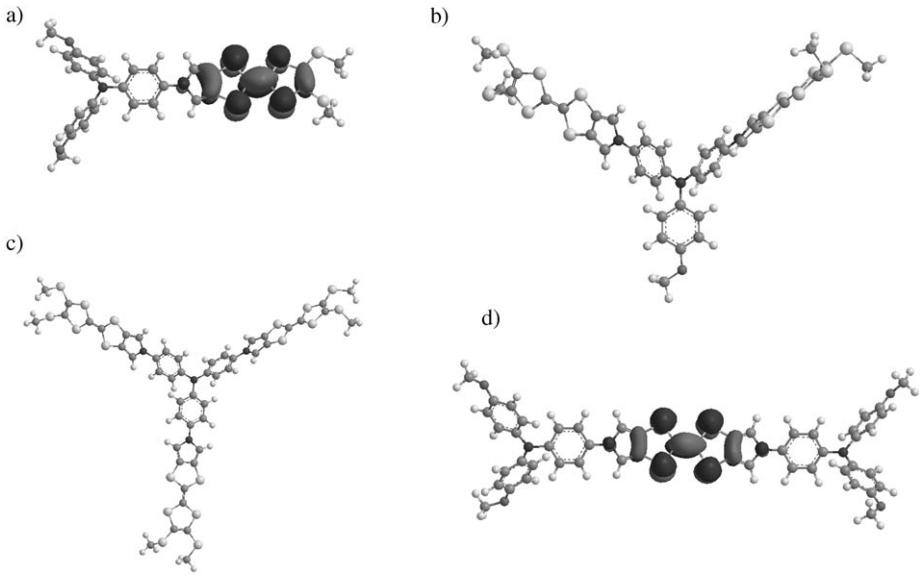

Figure 11. PM3-optimized geometries of **3**, **5**, **7**, and **9** (a) to d), respectively), and the corresponding HOMOs of **3** (a) and **9** (d). The long octylthio side chains have been replaced by methylthio groups for clarity.

 © 2006 Wiley-VCH Verlag GmbH & Co. KGaA, Weinheim

redox processes of the TTF and triarylamine moieties are reversible and occur in the region 0–1.0 V versus Fc/Fc^+. Based on the onset of oxidation, the HOMO energy levels are estimated to be about −4.7 eV, which is identical to that of TTF, and matches very well the work function of ITO (−4.7 eV). Although there is no significant electronic communication between the TTF moieties bridged by the triarylamine group (**5** and **7**), the redox behavior of the triarylamine group in **3**, **5**, and **7** is affected by the attachment of the TTF moieties: the redox potential of the triarylamine unit shifts to more positive values with increasing number of TTF propeller blades (**3** < **5** < **7**). Similarly, the interaction between terminal triarylamine groups is found to be very weak; however, the electronic interaction between the triarylamine and TTF groups is strong. The absorption spectra of the corresponding radical cations were studied in detail by chemical oxidant titration and spectroelectrochemical methods. All the results from the electrochemical investigations and the absorption spectra are mutually consistent. DSC demonstrates that compounds **5** and **7** are crystalline, while conjugate **9** forms a molecular glass with a clear glass transition. The PM3-optimized geometries suggest that the TTF moiety is almost coplanar with one phenyl ring of the triarylamine, and the large, rigid, planar blades of the propeller-shaped triarylamines facilitate intermolecular interactions that may result in crystalline materials. However, when the rigid TTF is capped with two three-dimensional triarylamine moieties, the interactions between the planar TTF are hindered and an amorphous solid results. Thus, conjugate **9** has a somewhat higher glass transition temperature than TPD (4,4′-bis(*m*-tolylphenylamino)biphenyl), T_g = 65 °C,[17e] at a significantly lower IP of 4.7 eV (TPD, IP = 5.38 eV).[24b]

In conclusion, our results suggest that the morphology of these TTF–triarylamine conjugates and the related electrooptical properties may be tuned by variation of the chemical structure. Further improvement of the glass transition temperature might be possible by rational design of molecular structures, for example, the introduction of more nonplanar groups, the incorporation of bulky and structurally rigid moieties, or increasing molecular size and weight.

Experimental Section

General: Reagents and solvents were purchased from Acros, Aldrich, and Fluka and were used as received. Dioxane was distilled from Na/benzophenone. MeCN was distilled from CaH_2. All reactions were carried out under a dry N_2 atmosphere.

^1H and ^{13}C NMR spectra were measured on a Bruker 400 MHz spectrometer. Chemical shifts are reported in ppm downfield from $SiMe_4$, using the solvent's residual signal as an internal reference. Coupling constants (*J*) are given in Hz. Resonance multiplicities are described as s (singlet), d (doublet), t (triplet), or m (multiplet). MALDI mass spectra were obtained on a Bruker Daltonics Autoflex II instrument using DCTB or dithranol as the matrix. All electrochemical investigations were carried out with a computer-controlled BAS CV50W potentiostat in dried and oxygen-free MeCN using 0.1 M tetrabutylammonium hexafluorophosphate ($TBAPF_6$) as supporting electrolyte, a platinum disk (Φ = 5 mm) as working electrode, a platinum wire as counter electrode, and an Ag/AgCl reference electrode. Redox potentials were referenced against ferrocene/ferrocenium (Fc/Fc^+). UV/Vis-NIR absorption spectra (in the chemical oxidant titration and spectroelectrochemistry investigations) were recorded with a Jasco V-750 spectrometer. In the chemical oxidant titrations, the concentration of the compounds was 2×10^{-5} M in CH_2Cl_2; spectra were measured from the solutions in a quartz cuvette of pathlength 1 cm after each stepwise addition of the oxidant $SbCl_5$ in CH_2Cl_2. Spectroelectrochemistry measurements were made in reflection mode with a Jasco V-750 spectrometer using a polished platinum disk working electrode in an electrochemical three-electrode cell controlled by a EG&G Model 363 potentiostat. Differential scanning calorimetry (DSC) studies of 1–2 mg samples of compounds **5, 7**, and **9** in sealed Al pans were performed on a Q1000 DSC system at a heating/cooling rate of 10 °C min^{-1} in a heat/cool/heat/cool mode. Bulk samples of compounds for DSC were prepared by slowly precipitating the compounds (purified by silica gel chromatography) from a mixture of petroleum ether/dichloromethane.

Preparation of 3: A flame-dried Schlenk reaction tube charged with a mixture of **2** (86 mg, 0.2 mmol), **1** (53 mg, 0.1 mmol), K_3PO_4 (63 mg), and CuI (6 mg) was degassed with N_2 for 10 min. After the addition of racemic *trans*-cyclohexanediamine (10 μL) and freshly distilled dioxane (2 mL) under N_2, the Schlenk tube was sealed and the reaction mixture was stirred while heating at 110 °C for 24 h. The mixture was then allowed to cool to room temperature and diluted with CH_2Cl_2. After successive washings with dilute aqueous ammonium hydroxide solution and water and drying over anhydrous $MgSO_4$, the crude product was purified by chromatography on silica gel using petroleum ether/dichloromethane (3:2) as eluent. Conjugate **3** was obtained as a yellow oil (38 mg; 46 % yield). ^1H NMR (400 MHz, CD_2Cl_2): δ = 7.02 (d, *J* = 9.0 Hz, 2H; ArH), 6.94 (d, *J* = 9.0 Hz, 4H; ArH), 6.84 (d, *J* = 9.0 Hz, 2H; ArH), 6.76 (d, *J* = 9.0 Hz, 4H; ArH), 6.73 (s, 2H; Py-H), 3.69 (s, 6H; OCH_3), 2.74 (t, *J* = 7.3 Hz, 4H; -SCH_2), 1.55 (m, *J* = 7.4 Hz, 4H; -$SCCH_2$), 1.40–1.10 (m, 20H; -SCH_2), 0.79 ppm (t, *J* = 7.0 Hz, 6H; -CH_3); ^{13}C NMR (400 MHz, CD_2Cl_2): δ = 159.47, 150.58, 143.90, 132.12, 130.88, 129.81, 129.70, 124.32, 123.96, 118.00, 117.86, 58.70, 39.54, 35.09, 33.08, 32.46, 32.35, 31.78, 25.92, 17.12 ppm; MALDI-MS: *m*/*z* calcd for $C_{44}H_{54}N_2O_2S_6$: 834.251; found: 834.209.

Preparation of 5: A flame-dried Schlenk reaction tube charged with a mixture of **4** (105.4 mg, 0.2 mmol), **1** (265.5 mg, 0.5 mmol), K_3PO_4 (233 mg), and CuI (10 mg) was degassed with N_2 for 10 min. After the addition of racemic *trans*-cyclohexanediamine (20 μL) and freshly distilled dioxane (2 mL) under N_2, the Schlenk tube was sealed and the reaction mixture was stirred while heating at 110 °C for 24 h. The mixture was then allowed to cool to room temperature and diluted with CH_2Cl_2. After successive washings with dilute aqueous ammonium hydroxide solution and water and drying over anhydrous $MgSO_4$, the crude product was purified by chromatography on silica gel using petroleum ether/dichloromethane (3:2) as eluent. Conjugate **5** was obtained as a yellow solid (88 mg; 33 % yield). ^1H NMR (400 MHz, CD_2Cl_2): δ = 7.10 (d, *J* = 8.8 Hz, 4H; ArH), 7.00 (m, 6H; ArH), 6.82 (d, *J* = 9.0 Hz, 2H; ArH), 6.78 (s, 4H; Py-H), 6.73 (s, 2H; Py-H), 3.72 (s, 3H; OCH_3), 2.75 (t, *J* = 7.3 Hz, 8H; -SCH_2), 1.55 (m, *J* = 7.4 Hz, 8H; -$SCCH_2$), 1.40–1.10 (m, 40H; -$SCC(CH_2)_5$), 0.79 ppm (t, *J* = 7.0 Hz, 12H; -CH_3); ^{13}C NMR (400 MHz, CD_2Cl_2): δ = 160.40, 149.31, 143.10, 138.08, 130.60, 126.71, 124.65, 118.17, 117.86, 58.65, 39.47, 35.00, 33.00, 32.38, 31.69, 25.83, 17.03 ppm; MALDI-MS: *m*/*z* calcd for $C_{67}H_{87}N_3OS_{12}$: 1333.350; found: 1333.357.

Preparation of 7: A flame-dried Schlenk reaction tube charged with a mixture of **6** (62 mg, 0.1 mmol), **1** (200 mg, 0.36 mmol), K_3PO_4 (200 mg), and CuI (7 mg) was degassed with N_2 for 10 min. After the addition of racemic *trans*-cyclohexanediamine (10 μL) and freshly distilled dioxane (2 mL) under N_2, the Schlenk tube was sealed and the reaction mixture was stirred while heating at 110 °C for 24 h. The mixture was then allowed to cool to room temperature and diluted with CH_2Cl_2. After successive washings with dilute aqueous ammonium hydroxide solution and water and drying over anhydrous $MgSO_4$, the crude product was purified by chromatography on silica gel using petroleum ether/dichloromethane

 © 2006 Wiley-VCH Verlag GmbH & Co. KGaA, Weinheim

(3:2) as eluent. Conjugate **7** was obtained as a yellow solid (73 mg; 40% yield). ^{1}H NMR (400 MHz, CD_2Cl_2): δ = 7.16 (d, J = 9.0 Hz, 6H; ArH), 7.07 (d, J = 9.0 Hz, 6H; ArH), 6.81 (s, 6H; ArH), 2.75 (t, J = 7.3 Hz, 12H; -SCH_2), 1.56 (m, J = 7.4 Hz, 12H; -$SCCH_2$), 1.40–1.10 (m, 60H; -SCH_2), 0.80 ppm (t, J = 7.0 Hz, 18H; -CH_3); ^{13}C NMR (400 MHz, CD_2Cl_2): δ = 147.62, 137.95, 129.88, 127.30, 124.09, 123.51, 113.33, 38.56, 34.11, 32.09, 31.48, 31.37, 30.80, 24.94, 16.14 ppm; MALDI-MS: m/z calcd for $C_{90}H_{120}N_4S_{18}$: 1832.449; found: 1832.432.

Preparation of 9: A flame-dried Schlenk reaction tube charged with a mixture of **2** (129.3 mg, 0.3 mmol), **8** (28.2 mg, 0.1 mmol), K_3PO_4 (106 mg), and CuI (5 mg) was degassed with N_2 for 10 min. After the addition of racemic *trans*-cyclohexanediamine (10 μL) and freshly distilled dioxane (2 mL) under N_2, the Schlenk tube was sealed and the reaction mixture was stirred while heating at 110°C for 24 h. The mixture was then allowed to cool to room temperature and diluted with CH_2Cl_2. After successive washings with dilute aqueous ammonium hydroxide solution and water and drying over anhydrous $MgSO_4$, the crude product was purified by chromatography on silica gel using petroleum ether/dichloromethane (3:2) as eluent. Conjugate **9** was obtained as a yellow solid (46.2 mg; 52% yield). ^{1}H NMR (400 MHz, CD_2Cl_2): δ = 7.04 (d, J = 9.0 Hz, 4H; ArH), 6.94 (d, J = 9.0 Hz, 8H; ArH), 6.85 (d, J = 9.0 Hz, 4H; ArH), 6.75 (m, 12H; ArH and Py-H), 3.69 ppm (s, 12H; OCH_3); ^{13}C NMR (400 MHz, CD_2Cl_2): δ = 159.35, 150.43, 143.84, 135.18, 129.70, 124.27, 124.17, 117.85, 58.61 ppm; MALDI-MS: m/z calcd for $C_{50}H_{40}N_4O_4S_4$: 888.193; found: 888.193.

Acknowledgements

We are grateful to the Deutsche Forschungsgemeinschaft for financial support. H. Li thanks the Alexander von Humboldt Foundation for a research grant. We also thank Prof. F. Würthner and A.-M. Krause for the DSC measurements, and S. Amthor for help with the PM3 optimizations.

[1] J. P. Ferraris, D. O. Cowan, V. Walatka, J. H. Perlstein, *J. Am. Chem. Soc.* **1973**, *95*, 43.

[2] a) See the special issue on molecular conductors: *Chem. Rev.* **2004**, *104*, 4887–5781; b) J. M. Williams, J. R. Ferraro, R. J. Thorn, K. D. Carlson, U. Geiser, H. H. Wang, A. M. Kini, M.-H. Whangbo, *Organic Superconductors (including fullerenes)*, Prentice Hall, Englewood Cliffs, NJ, **1992**; c) T. Ishiguro, K. Yamaji, G. Saito, *Organic Superconductors*, 2nd ed., Springer, Berlin, **1998**.

[3] a) G. Schukat, E. Fanghänel, *Sulfur Rep.* **1996**, *18*, 1; b) J. Garín, *Adv. Heterocycl. Chem.* **1995**, *62*, 249; c) K. B. Simonsen, N. Svenstrup, J. Lau, O. Simonsen, P. Mørk, G. J. Kristensen, J. Becher, *Synthesis* **1996**, 407; d) J.-I. Yamada, H. Nishikawa, K. Kikuchi, *J. Mater. Chem.* **1999**, *9*, 617; e) J. J. Novoa, M. C. Rovira, C. Rovira, J. Veciana, J. Tarrs, *Adv. Mater.* **1995**, *7*, 233; f) E. M. Engler, V. V. Patel, *J. Am. Chem. Soc.* **1974**, *96*, 7376; g) R. D. McCullough, G. B. Kok, K. A. Lerstrup, D. O. Cowan, *J. Am. Chem. Soc.* **1987**, *109*, 4115; h) M. Mizuno, A. F. Garito, M. P. Cava, *J. Chem. Soc. Chem. Commun.* **1978**, 18.

[4] a) P. Frère, P. J. Skabara, *Chem. Soc. Rev.* **2005**, *34*, 69, and references therein; b) M. Iyoda, M. Hasegawa, Y. Miyake, *Chem. Rev.* **2004**, *104*, 508; c) J. Roncali, *J. Mater. Chem.* **1997**, *7*, 2307.

[5] M. Fourmigu, P. Batail, *Chem. Rev.* **2004**, *104*, 5379, and references therein.

[6] a) J. L. Segura, N. Martín, *Angew. Chem.* **2001**, *113*, 1416; *Angew. Chem. Int. Ed.* **2001**, *40*, 1372; b) J. O. Jeppesen, M. B. Nielsen, J. Becher, *Chem. Rev.* **2004**, *104*, 5115; c) M. R. Bryce, W. Davenport, L. M. Goldenberg, C. Wang, *Chem. Commun.* **1998**, 945; d) T. Jørgensen, T. K. Hansen, J. Becher, *Chem. Soc. Rev.* **1994**, *23*, 41; e) K. B. Simonsen, J. Becher, *Synlett* **1997**, 1211.

[7] a) P. L. Boulas, M. Gomez-Kaifer, L. Echegoyen, *Angew. Chem.* **1998**, *110*, 226; *Angew. Chem. Int. Ed.* **1998**, *37*, 216; b) G. Trippé, E. Levillain, F. Le Derf, A. Gorgues, M. Sallé, J. O. Jeppesen, K. Nielsen, J. Becher, *Org. Lett.* **2002**, *4*, 2461; c) K. A. Nielsen, J. O. Jeppesen, E. Levillain, J. Becher, *Angew. Chem.* **2003**, *115*, 197; *Angew. Chem. Int. Ed.* **2003**, *42*, 187.

[8] a) H. Li, J. O. Jeppesen, E. Levillain, J. Becher, *Chem. Commun.* **2003**, 846; b) P. R. Ashton, V. Balzani, J. Becher, A. Credi, M. C. T. Fyfe, G. Mattersteig, S. Menzer, M. B. Nielsen, F. M. Raymo, J. F. Stoddart, M. Venturi, D. J. Williams, *J. Am. Chem. Soc.* **1999**, *121*, 3951; c) V. Balzani, A. Credi, G. Mattersteig, O. A. Mathews, F. M. Raymo, J. F. Stoddart, M. Venturi, A. J. P. White, D. J. Williams, *J. Org. Chem.* **2000**, *65*, 1924.

[9] a) D. Philp, A. M. Z. Slavin, N. Spencer, J. F. Stoddart, D. J. Williams, *J. Chem. Soc. Chem. Commun.* **1991**, 1584; b) J. O. Jeppesen, J. Perkins, J. Becher, J. F. Stoddart, *Angew. Chem.* **2001**, *113*, 1256; *Angew. Chem. Int. Ed.* **2001**, *40*, 1216; c) J. O. Jeppesen, K. A. Nielsen, J. Perkins, S. A. Vignon, D. DiFabio, R. Ballardini, M. T. Gandolfi, M. Venturi, V. Balzani, J. Becher, J. F. Stoddart, *Chem. Eur. J.* **2003**, *9*, 2982.

[10] a) C. Kollmar, O. Kahn, *Acc. Chem. Res.* **1993**, *26*, 259; b) R. Kumai, M. M. Matsushita, A. Izuoka, T. Sugawara, *J. Am. Chem. Soc.* **1994**, *116*, 4523; c) H. Mizouchi, A. Ikawa, H. Fukutome, *J. Am. Chem. Soc.* **1995**, *117*, 3260; d) R. D. McCullough, J. A. Belot, A. L. Rheingold, G. P. A. Yap, *J. Am. Chem. Soc.* **1995**, *117*, 9913; e) T. Enoki, A. Miyazaki, *Chem. Rev.* **2004**, *104*, 5449.

[11] a) A. Aviram, M. Ratner, *Chem. Phys. Lett.* **1974**, *29*, 2271; b) R. M. Metzger, *J. Mater. Chem.* **1999**, *9*, 2027; c) R. M. Metzger, *Acc. Chem. Res.* **1999**, *32*, 950; d) G. Ho, J. R. Heath, M. Kondratenko, D. F. Perepichka, K. Arseneault, M. Pézolet, M. R. Bryce, *Chem. Eur. J.* **2005**, *11*, 2914.

[12] a) M. Mas-Torrent, M. Durkut, P. Hadley, X. Ribas, C. Rovira, *J. Am. Chem. Soc.* **2004**, *126*, 984; b) S. T. Bromley, M. Mas-Torrent, P. Hadley, C. Rovira, *J. Am. Chem. Soc.* **2004**, *126*, 6544.

[13] a) A. I. De Lucas, N. Martín, L. Sánchez, C. Seoane, R. Andreu, J. Garín, J. Orduna, R. Alcalá, B. Villacampa, *Tetrahedron* **1998**, *54*, 4655; b) M. González, N. Martín, J. L. Segura, C. Seoane, J. Garín, J. Orduna, R. Alcalá, C. Sánchez, B. Villacampa, *Tetrahedron Lett.* **1999**, *40*, 8599; c) J. A. Hansen, J. Becher, J. O. Jeppesen, E. Levillain, M. B. Nielsen, B. M. Petersen, J. C. Petersen, Y. Sahin, *J. Mater. Chem.* **2004**, *14*, 179.

[14] a) M. Prato, M. Maggini, C. Giacometti, G. Scorrano, G. Sandon, G. Farnia, *Tetrahedron* **1996**, *52*, 5221; b) N. Martín, L. Sánchez, C. Seoane, R. Andreu, J. Garín, J. Orduna, *Tetrahedron Lett.* **1996**, *37*, 5979; c) N. Martín, L. Sánchez, D. M. Guldi, *Chem. Commun.* **2000**, 113.

[15] a) M. Thelakkat, *Macromol. Mater. Eng.* **2002**, *287*, 442; b) A. Facchetti, M.-H. Yoon, T. J. Marks, *Adv. Mater.* **2005**, *17*, 1705; c) Y. Shirota, *J. Mater. Chem.* **2000**, *10*, 1; d) M. Sonntag, K. Kreger, D. Hanft, P. Strohriegl, S. Setayesh, D. Leeuw, *Chem. Mater.* **2005**, *17*, 3031.

[16] a) Y. Shirota, *J. Mater. Chem.* **2005**, *15*, 75; b) P. Strohriegl, J. V. Grazulevicius, *Adv. Mater.* **2002**, *14*, 1439.

[17] a) A. N. Sobolev, V. K. Belsky, I. P. Romm, N. Y. Chermikova, E. N. Guryanova, *Acta Crystallogr. Sect. C* **1985**, *C41*, 967; b) H. B. Lueck, J. L. McHale, W. D. Edwards, *J. Am. Chem. Soc.* **1992**, *114*, 2342; c) M. Malagoli, J. L. Brédas, *Chem. Phys. Lett.* **2000**, *327*, 13; d) I. Reva, L. Lapinski, N. Chattopadhyay, R. Fausto, *Phys. Chem. Chem. Phys.* **2003**, *5*, 3844; e) B. E. Koene, D. E. Loy, M. E. Thompson, *Chem. Mater.* **1998**, *10*, 2235.

[18] a) K. Okumoto, Y. Shirota, *Chem. Lett.* **2000**, 1034; b) J. Salbeck, F. Weissörtel, *Macromol. Symp.* **1997**, *125*, 121; c) Y. Shirota, S. Nomura, H. Kageyama, *Proc. SPIE-Int. Soc. Opt. Eng.* **1998**, *3476*, 132; d) C. Hohle, P. Strohriegl, S. Schloter, U. Hofmann, D. Haarer, *Proc. SPIE-Int. Soc. Opt. Eng.* **1998**, *3471*, 29; e) P. Strohriegl, J. V. Grazulevicius, *Adv. Mater.* **2002**, *14*, 1439.

[19] M. R. Bryce, *Adv. Mater.* **1999**, *11*, 11.

[20] Y. Shirota, T. Tomokazu, N. Noma, *Chem. Lett.* **1989**, *7*, 1145.

[21] J. O. Jeppesen, K. Takimiya, F. Jensen, T. Brimert, K. Nielsen, N. Thorup, J. Becher, *J. Org. Chem.* **2000**, *65*, 5794.

[22] A. Klapars, J. C. Antilla, X. Huang, S. L. Buchwald, *J. Am. Chem. Soc.* **2001**, *123*, 7727.

[23] M. Thelakkat, H.-W. Schmidt, *Adv. Mater.* **1998**, *10*, 219.

 © 2006 Wiley-VCH Verlag GmbH & Co. KGaA, Weinheim

[24] The ionization potential (IP) of triphenylamine was reported to be 6.8 eV, as estimated from gas-phase ultraviolet photoelectron spectroscopy (UV-PES). However, the IP (or HOMO) of condensed triarylamines is much lower. See: a) *NIST Chemistry WebBook*, *NIST Standard Reference Database Number 69* (Eds.: P. J. Linstrom, W. G. Mallard), National Institute of Standards and Technology, Gaithersburg MD, 20899, June **2005** (http://webbook.nist.gov); b) J. D. Anderson, E. M. McDonald, P. A. Lee, M. L. Anderson, E. L. Ritchie, H. K. Hall, T. Hopkins, E. A. Mash, J. Wang, A. Padias, S. Thayumanavan, S. Barlow, S. R. Marder, G. E. Jabbour, S. Shaheen, B. Kippelen, N. Peyghambarian, R. M. Wightman, N. R. Armstrong, *J. Am. Chem. Soc.* **1998**, *120*, 9646.

[25] K. Zimmer, B. Gödicke, M. Hoppmeier, H. Mayer, A. Schweig, *Chem. Phys.* **1999**, *248*, 263.

[26] S. Amthor, C. Lambert, *Chem. Phys.* **2005**, available from the web as article in press.

[27] C. Lambert, S. Amthor, J. Schelter, *J. Phys. Chem. A* **2004**, *108*, 6474.

[28] a) C. Loosli, C. Jia, S.-X. Liu, M. Haas, M. Dias, E. Levillain, A. Neels, G. Labat, A. Hauser, S. Decurtins, *J. Org. Chem.* **2005**, *70*, 4988; b) H. Li, J. O. Jeppesen, E. Levillain, J. Becher, *Chem. Commun.* **2003**, 846; c) C. Wang, M. R. Bryce, A. S. Batsanov, C. F. Stanley, A. Beeby, J. A. K. Howard, *J. Chem. Soc. Perkin Trans. 2* **1997**, 1671.

Received: August 1, 2005
Published online: October 27, 2005

 © 2006 Wiley-VCH Verlag GmbH & Co. KGaA, Weinheim